Progress In Electromagnetics Research M, Vol. 90, 59–67, 2020

Optimization of Wide-Band and Wide Angle Cavity-Backed Microstrip Patch Array Using Genetic Algorithm

Doo-Soo Kim[3, *], Il-Tak Han[1], Woo-Sung Kim[1], Jin-Mo Yang[1], Yong-Hee Han[2], and Kyung-Tae Kim[3]

Abstract—This paper specifies optimization of a low active reflection coefficient (ARC) array element with a cavity-backed microstrip patch (CBMP) using a genetic algorithm (GA) at wide-band and 2-dimensional (2D) wide angle. Both the GA implemented with a user-defined MATLAB code and a 3-dimensional (3D) full-wave electromagnetic simulator CST MWS are simulated with a real-time direct link. An optimization method using not a traditional unit cell or a small array but a 15×15 finite array structure is proposed to apply to a large-scale array antenna. The CBMP array antenna to meet a design goal of a max ARC is optimally designed at equally divided 9 frequencies and 11374 beam angles for S-band 400 MHz operating frequency bandwidth and beam scan coverage ($\mathrm{Az} = -60^\circ \sim +60^\circ$, $\mathrm{El} = -3^\circ \sim +90^\circ$). Measurement results show that a prototype and a full-scale array antenna have low ARC below -8.1 dB and -6.9 dB, respectively for required wide frequency bandwidth and beam scan coverage. It is confirmed that the proposed method is a good solution for optimizing a large-scale array antenna.

1. INTRODUCTION

Recently, radars play an important role in detection, tracking, and identification of small targets in severe jamming and clutter environments with wide-band and 2D wide beam scan coverage. Therefore, a low loss active electronically scanned array (AESA) antenna consisting of hundreds or thousands of array elements is a core hardware technology, and ARC generated at wide-band and wide angle becomes a key factor for radar performance. A high ARC causes a lot of damage of transmit/receive module and a considerable gain loss of the AESA antenna. In this regard, a design of a low ARC array element for an AESA antenna is a critical topic. Currently, researches of an array element suitable for wide-band and wide angle are carried out restrictively. In [1, 2], low ARC characteristic is discussed for a probe-fed stacked microstrip patch and a CBMP in a unit cell and a small array for wide-band and 1D beam scan coverage. These focus on the improvement of ARC at wide band for restrictive beam scan coverage such as a bore-sight and principle plane. Also some researches are carried out to improve the ARC by applying various parasitic structures and an electromagnetic band gap (EBG) shape to reduce the mutual coupling between array elements [3–5]. These additional structures increase spatial constraint and manufacture complexity of a large-scale array antenna, so optimization of the array element without additional structures should be carried out for wide-band and 2D wide beam coverage.

Generally, particle swarm optimization (PSO) and genetic algorithm (GA) are most frequently used in optimization. PSO is recently applied in various types of array antennas for broadband, reconfigurable and switched-beam applications [6–9] and used in conjunction with CST MWS to design near-field correcting structures and spatial phase shifters [10, 11]. Also this data-driven optimization is

Received 28 December 2019, Accepted 15 February 2020, Scheduled 4 March 2020
* Corresponding author: Doo-Soo Kim (dskim@add.re.kr).
[1] Agency for Defense Development, Daejeon, Korea. [2] Hanhwa Systems, Yong-in, Korea. [3] Electronic and Electrical Engineering, Pohang University of Science and Technology, Pohang, Korea.

implemented to design various types of EM or microwave devices such as couplers, frequency selective surfaces, artificial magnetic conductors, aperture distribution, and filters [12–17]. However, it is not easy to find that the data-driven optimization is used to design large-scale array antennas. GA is one of the efficient and popular optimization algorithms in convergence speed and global optimal solution [18]. A design of the array element using GA almost focuses on side-lobe level (SLL) reduction, beam broadening, and null steering for adaptive beam forming [19–21]. Also optimization of array elements such as a slot, a log periodic element, and a microstrip patch is done by using a GA toolbox offered from HFSS and CST MWS to improve axial ratio, gain, SLL, and ARC [22–24]. Generally, the design to optimize the array element by using GA toolbox is considerably restricted for multiple frequencies and beam scan angles. The more frequencies and beam scan angles are, the more impossible optimization using the GA toolbox is.

This paper handles optimization of a large-scale low ARC CBMP array antenna without additional structures for wide-band and 2D wide beam scan coverage by using the GA. Both the GA implemented with a user-defined MATLAB code and a 3-dimensional (3D) full-wave electromagnetic simulator CST MWS are simulated with a real-time direct link. Optimization for design parameters of a CBMP array element suitable for large-scale array antennas is carried out to minimize a max ARC, cost function, at multiple frequencies and beam scan angles.

2. ANTENNA STRUCTURE

2.1. Cavity-Backed Microstrip Patch (CBMP)

Figure 1 shows a 15×15 array structure and an array element. The array element consists of a radome, a cavity-backed microstrip patch (CBMP), and a spacer. A honeycomb in the radome is sandwiched between two FRP (Fiber glass) plates considering structural robustness and signal loss. A cavity-backed feed structure is applied to a microstrip patch antenna to implement a wide-band frequency characteristic. Main design parameters of the CBMP to determine a frequency resonance are patch size, feed offset, probe radius, and inner cavity size. Especially probe radius and feed offset are sensitive to the frequency resonance and should be handled carefully. An ARC of a phased array antenna is important, and a design to reduce both self-reflection and a coupling coefficient between array elements should be carried out. To maintain flatness for high precision beam accuracy of the array antenna, a PEI foam is placed between the radome and the CBMP.

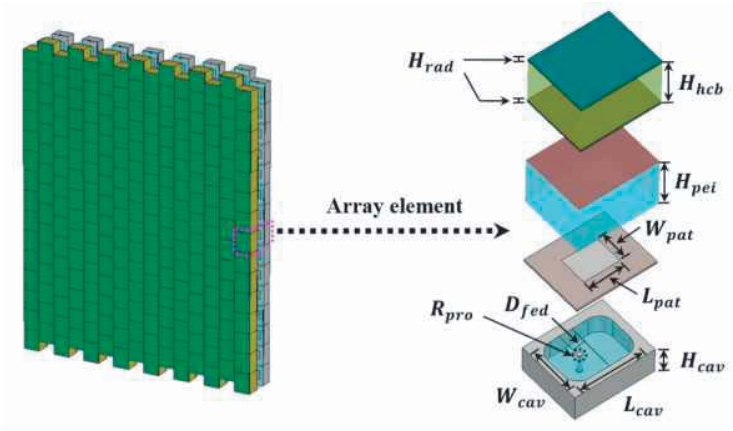

Figure 1. 15×15 array structure and array element.

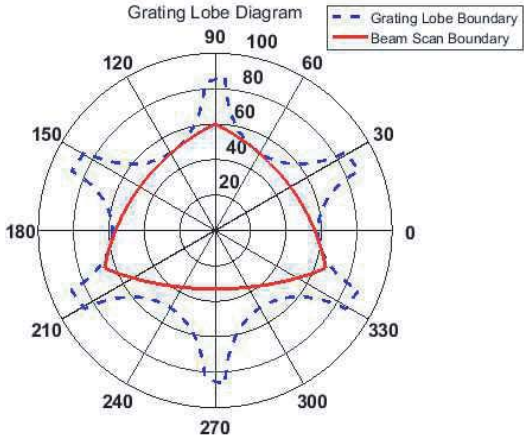

Figure 2. Grating lobe diagram.

2.2. 15×15 Array Prototype

It is common to manufacture, test, and verify a prototype prior to a full-scale array antenna. Considering convergence of an ARC for S-band 400 MHz frequency bandwidth and beam scan coverage, the number

of array elements is selected as 15×15 with increase of array elements from 5×5 to 21×21. Array element distances in horizontal and vertical directions are $0.51\lambda_c$ and $0.62\lambda_c$, respectively.

3. OPTIMIZATION

3.1. Grating Lobe Diagram/Active Reflection Coefficient (ARC)

Figure 2 shows a grating lobe diagram of a designed array antenna in spherical coordinate. A maximum operating frequency, a beam scan coverage, and an antenna tilt angle (30°) are used. The dotted line is a grating lobe boundary calculated with the array element distance, and the dashed line is a beam scan boundary. Eq. (1) describes an ARC formula of the m-th array element in a planar array consisting of M and N elements in horizontal and vertical directions, respectively. The ARC is a function including frequency (f), theta (θ). and phi (ϕ). $S_{n,m}$ is S-parameter of the m-th array element that is a feeding element, and $x_{p,n}$, $x_{p,m}$, $y_{p,n}$ and $y_{p,m}$ are positions of the m-th and n-th array elements in horizontal and vertical directions, respectively.

$$ARC_m(\theta, \phi, f) = \sum_{n=1}^{MN} S_{n,m} \cdot e^{-j\frac{2\pi f}{c}[(x_{p,n}-x_{p,m})\sin\theta\cos\phi+(y_{p,n}-y_{p,m})\sin\theta\sin\phi]} \quad (1)$$

3.2. Optimization Process

Figure 3 shows an optimization flowchart devised to design a 15×15 CBMP array antenna using GA. This flowchart includes co-simulation between the GA implemented with a user-defined MATLAB code and a 3D full-wave EM simulator CST MWS to optimize a low ARC 15×15 CBMP array antenna. The GA handles design parameters of the 15×15 CBMP array antenna and carries out cost calculation for ARC, evaluation, and children generation. CST MWS calculates S-parameters among 225 elements and receives updated design parameters from the GA. This process is iteratively carried out depending on a design goal or user's constraints.

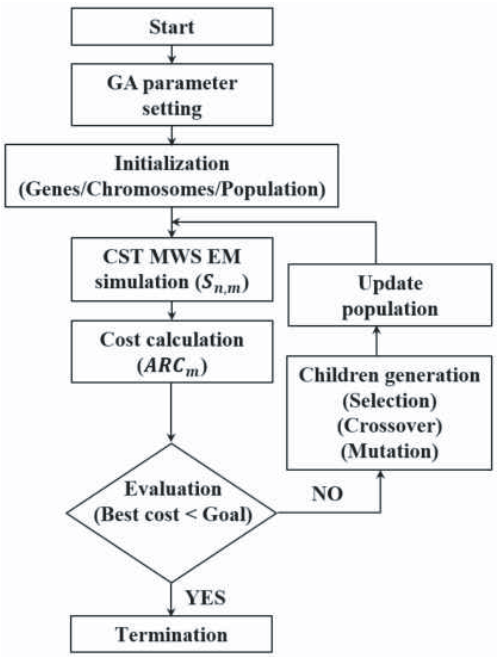

Figure 3. Optimization flowchart.

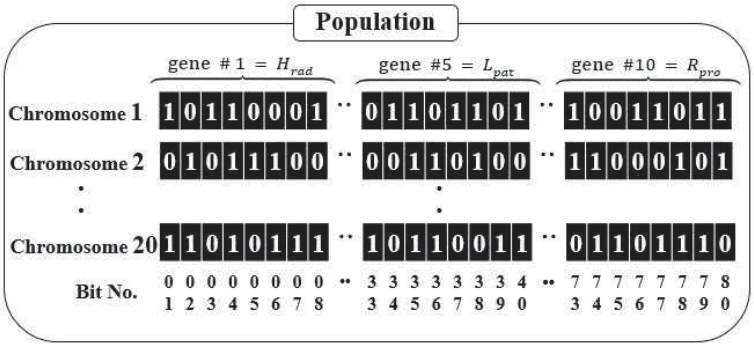

Figure 4. Genes/Chromosomes/Population.

3.2.1. GA Parameter Setting/Initialization

GA parameters consist of a gene, a chromosome, population, a generation, and a design goal. The gene is selected as 8 bits that represent enough step from min to max values of design parameters. The chromosome is selected as 10 that is the number of design parameters as shown in Figure 1. The design parameters to optimize a 15×15 CBMP array antenna are 10 as H_{rad}, H_{hcb}, H_{pei}, W_{pat}, L_{pat}, H_{cav}, W_{cav}, L_{cav}, D_{fed}, and R_{pro}. Considering calculation time of CST MWS, population is selected as 20 chromosomes, and the number of chromosomes to survive after each iteration is 10. The max number of generations to terminate GA is 120 considering calculation time of each iteration. The design goal allows ARC below -8 dB for operating frequency bandwidth and 2D beam scan coverage. At initialization, quantized genes, chromosomes, and population are generated as shown in Figure 4. Each chromosome consists of total 80 bits, and each gene has a value of 256 steps.

3.2.2. Cost Calculation/Evaluation

Figure 5 shows a data link between GA and CST MWS. As shown in Figure 4, a 80-bits chromosome generated from 10 design parameters is converted into a real value and delivered to CST MWS. *S*-parameters, consisting of a self-reflection coefficient and coupling coefficients from 224 adjacent elements, are calculated through EM analysis for a 15×15 CBMP array antenna. A graphic processing unit (GPU) is used to improve calculation speed for analyzing about 100 million meshes. Calculated 225 *S*-parameters are delivered to GA and used as input data to calculate cost by using Eqs. (1) and (2). As shown in Figure 5, a cost function includes 9 frequencies and 11374 beam scan angles with 50 MHz and 1 degree equally spaced respectively. Max ARC for 9 frequencies and 11374 beam scan angles becomes the cost of a corresponding chromosome. Costs of all chromosomes are sorted in ascending order and evaluated whether a design goal (< -8 dB) is satisfied or not. In Eq. (2), conv means coordinate

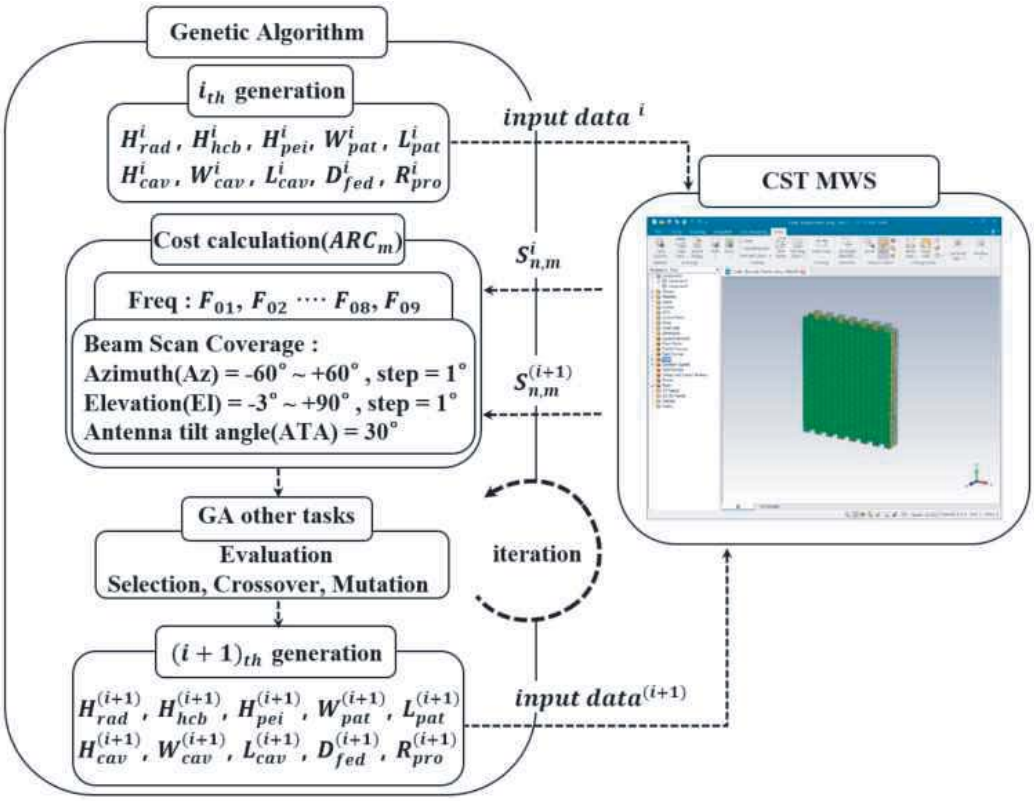

Figure 5. Data link between GA and CST MWS.

conversion.

$$Cost\ function = \underbrace{\max}_{f\in F_N}\{\ \underbrace{\max}_{\substack{(Az,El)\rightarrow \\ conv(\theta,\phi)}}\ \{ARC_m(\theta,\phi,f)\}\} \tag{2}$$

$$for\ 1 \le N \le 9,\quad -60^\circ \le Az \le +60^\circ,\quad -3^\circ \le El \le +90^\circ\ at\ ATA = 30^\circ$$

3.2.3. Children Generation

After cost calculation and evaluation, survived top 10 chromosomes in ascending order generate children chromosomes. A high rank chromosome has high probability of selection for children chromosomes. Selected parent chromosomes generate children chromosomes with single-point crossover that is formed as a random bit string. And a mutation rate is 0.02. We use the standard GA to carry out optimization.

3.3. Design Results

Figure 6 shows the best cost of each generation with GA operated iteratively. A final design goal is not satisfied, and the max number of generations set to terminate GA is carried out. As shown in Figure 6, total 4 rapid cost variations occur, and the variation rate is decreased as the number of generations increases. The final best cost for 120 generations is -7.7, and Table 1 describes values of optimized 10 design parameters of a 15×15 CBMP array antenna.

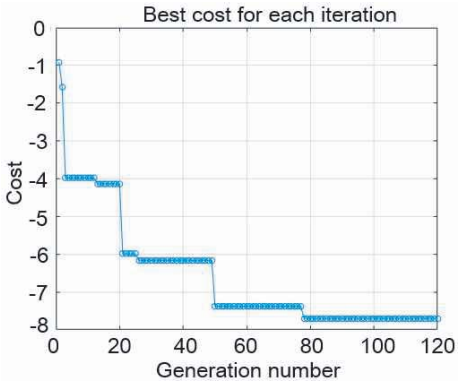

Figure 6. Best cost with GA.

Table 1. Optimized design parameters.

Design Parameter	Value (λ_c)	Design Parameter	Value (λ_c)
H_{rad}	0.011	H_{cav}	0.137
H_{hcb}	0.416	W_{cav}	0.445
H_{pei}	0.384	L_{cav}	0.533
W_{pat}	0.288	D_{fed}	0.082
L_{pat}	0.273	R_{pro}	0.018

Figure 7 shows design results of a center element of optimized 15×15 CBMP array antenna. Max ARC for beam scan coverage at each frequency is shown in Figure 7(a), and the best cost in Figure 6 is the same as max ARC of F02. Except F02, max ARC at each frequency is below -8 dB. The ARC for beam scan coverage at center frequency F05 shown in Figure 7(b) is symmetrical and considerably low below -10 dB. Max ARC for beam scan coverage is -10.38 dB at (Az, El) $= (-60^\circ, 4^\circ)$ which is placed at a beam scan boundary. Beam patterns of the center element at F05 are shown in Figure 7(c). The coupling from adjacent elements seems to generate ripples in beam patterns.

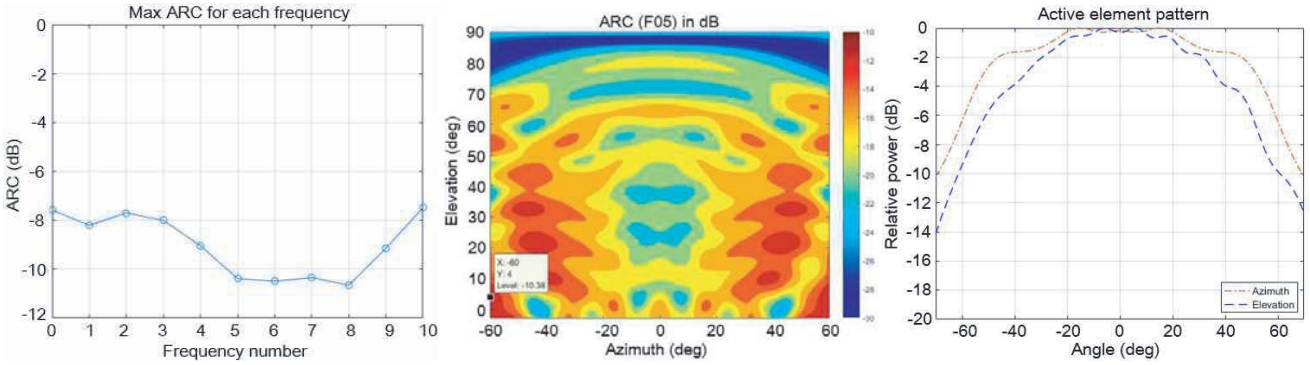

(a) (b) (c)

Figure 7. Optimized design results of CBMP 15×15 array antenna. (a) Max ARC at each frequency. (b) ARC of F05 for beam scan coverage. (c) Active element beam patterns.

4. MANUFACTURE & MEASUREMENT

4.1. Prototype

Figure 8 shows a manufactured 15×15 CBMP array antenna. As shown in Figure 8(a), a 15×15 microstrip patch array consists of 3 pieces in vertical direction and is assembled with a cavity structure. The PCB material for microstrip patch array is TLE-95 ($\varepsilon_r = 2.95$, $\tan\delta = 0.0026$). A room temperature film is placed to bond the microstrip patch array and the cavity structure, and a compressor is used for 12 hours to maintain a vacuum state between them. As explained in Figure 1, a honeycomb in a radome is sandwiched between two FRP plates and bonded to them with a high temperature film in an autoclave facility. The radome is assembled to the cavity structure with surrounding FRP frames.

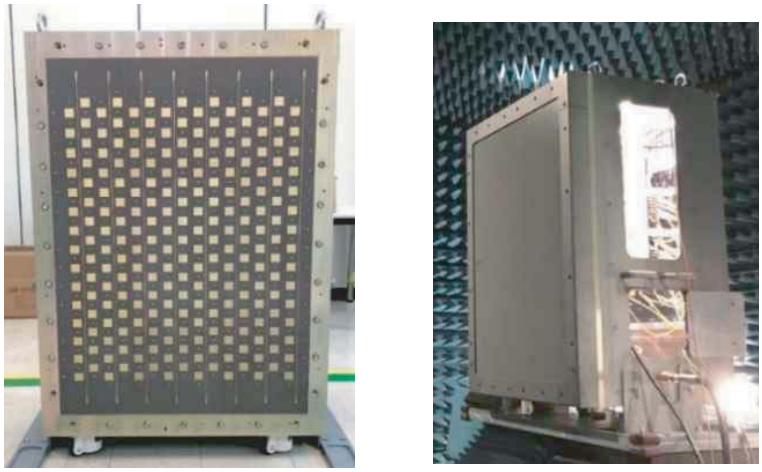

(a) (b)

Figure 8. Manufactured 15×15 CBMP array antenna. (a) Without radome. (b) With radome.

Figure 9 shows measurement results of a center element of optimized 15×15 CBMP array antenna. Max ARC for beam scan coverage at each frequency is shown in Figure 9(a). Within operating frequency bandwidth, F02 and F09 have -8.2 and -8.1 dB of max ARC, respectively. Max ARC at each frequency except two frequencies is below -9 dB. Compared with design results, max ARC of measurement results is generated with 50 MHz shifted to a lower frequency. It seems to be caused by a position error of a probe feed in bonding process between the cavity structure and 3 pieces microstrip patch array. As

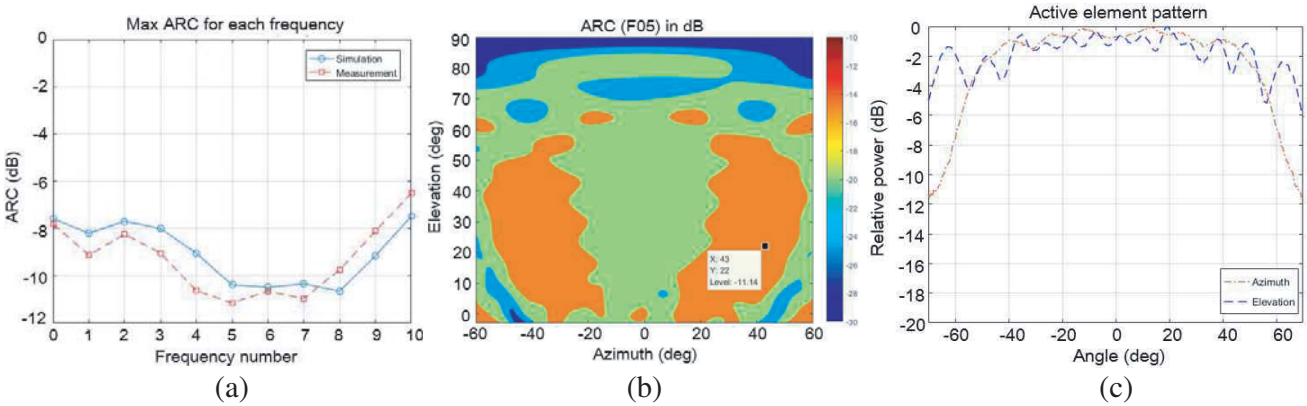

(a) (b) (c)

Figure 9. Measurement results of CBMP 15×15 array antenna. (a) Max ARC at each frequency. (b) ARC of F05 for beam scan coverage. (c) Active element beam patterns.

explained earlier, feed offset is sensitive to the frequency resonance. Also a thickness error of a bonding film between them seems to cause a frequency shift of max ARC. The ARC for beam scan coverage at F05 shown in Figure 9(b) is a little non-symmetrical and considerably low below -11 dB. Max ARC for beam scan coverage is -11.14 dB at (Az, El) = (43°, 22°). Beam patterns of a center element at F05 are shown in Figure 9(c), which are measured in a far-field anechoic chamber.

4.2. Full-Scale Array Antenna

Figure 10 shows a manufactured full-scale CBMP array antenna and measurement results. As shown in Figure 10(a), an array antenna consists of 48 columns and 28 rows, and the number of array elements is 1152. Five circle sections to measure ARC are depicted in Figure 10(b). Each section includes a 15×15 CBMP array antenna to compare with both design results and prototype measurements. Measurement results of the full-scale CBMP array antenna are shown in Figure 10(c). Max ARC for beam scan coverage at each frequency on each section is shown. Within operating frequency bandwidth, both F02 and F09 have -6.9 dB of max ARC. Max ARC at each frequency except two frequencies is below -7.3 dB. Compared with prototype results in Figure 9(a), relatively high max ARC seems to be caused by different array sizes between a prototype and a full-scale array. Also an ARC variation of five sections at high frequencies (F08, F09) seems to come from uneven position error of probe feeds and nonuniform thickness of bonding film among sections. On the other hand, a max ARC variation

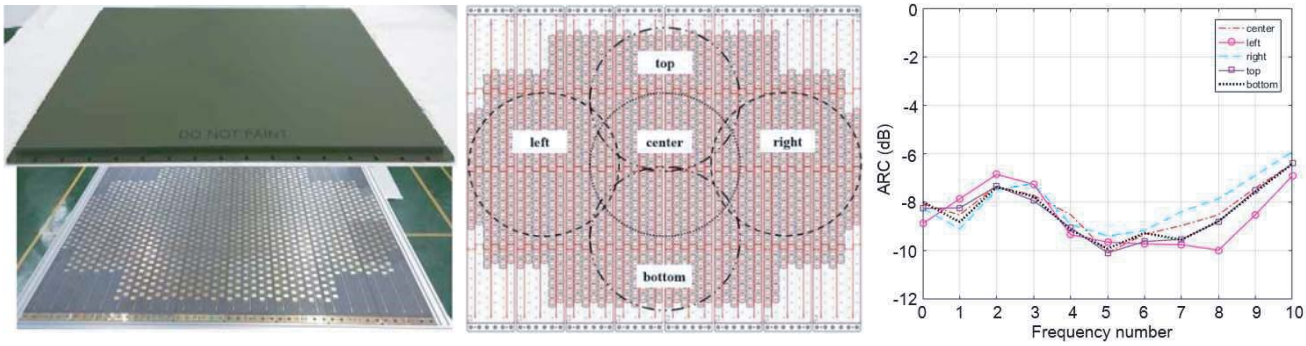

(a) (b) (c)

Figure 10. Full-scale array antenna structure and measurement results. (a) Manufactured full-scale CBMP array antenna. (b) 15×15 array antenna sections to measure ARC. (c) Max ARC at each frequency for 5 sections.

trend of each section is similar to that of a prototype. Although they are not shown here from lack of space, beam patterns of the full-scale CBMP array antenna are also measured in a large-scale near-field anechoic chamber. With wide-band and wide angle CBMP array designed, high gain and low side lobe beams to satisfy high precision beam accuracy are confirmed.

5. CONCLUSION

This paper specifies an optimized low ARC CBMP array antenna for S-band 400 MHz operating frequency bandwidth and 2D beam scan coverage (Az $= -60° \sim +60°$, El $= -3° \sim +90°$) by using GA. Generally to optimize large-scale array antennas for multiple frequencies and beam scan angles is considerably restricted when GA toolbox offered from a 3D full-wave EM simulator is used. In this paper, the GA implemented with a user-defined MATLAB code and the 3D full-wave EM simulator CST MWS are co-simulated with a real-time direct link. Optimization method using not a traditional unit cell or a small array but a 15×15 finite array structure is proposed to apply to a large-scale array antenna. The CBMP array antenna to meet a design goal of max ARC is optimally designed for equally divided 9 frequencies and 11374 beam angles by using GA. Measurement results show that a prototype and a full-scale array antenna have a low ARC below -8.1 dB and -6.9 dB respectively for required wide frequency bandwidth and beam scan coverage. It is confirmed that the proposed method is a good solution for optimizing large-scale array antennas.

REFERENCES

1. Waterhouse, R. B., "Design and scan performance of large, probe-fed stacked microstrip patch arrays,", *IEEE Transactions on Antennas and Propagation*, Vol. 50, 893–895, 2002.
2. Aza, G. and M. A. Zapata, "Broad-band cavity-backed and capacitively probe-fed microstrip patch arrays," *IEEE Transactions on Antennas and Propagation*, Vol. 48, 784–789, 2000.
3. Biswal, S. P. and S. Das, "Mutual coupling reduction of a printed dual element antenna system using a parasitic scatter," *2018 IEEE International Symposium on Antennas and Propagation & USNC/URSI National Radio Science Meeting*, 1375–1376, 2018.
4. Dominguez, G. E., J. F. Gonzalez, P. Padilla, and M. S. Castaner, "Mutual coupling reduction using EBG in steering antennas," *IEEE Antennas and Wireless Propagation Letters*, Vol. 11 1265–1268, 2012
5. Lee, J. Y., S. H. Kim, and J. H. Jang, "Reduction of mutual coupling in planar multiple antenna by using 1-D EBG and SRR structures," *IEEE Transactions on Antennas and Propagation*, Vol. 63, 4194–4198, 2015.
6. Caorsi, S., M. Donelli, A. Lommi, and A. Massa, "Location and imaging of two-dimensional scatterers by using a particle swarm algorithm," *Journal of Electromagnetic Waves and Applications*, Vol. 18, No. 4, 481–494, 2004.
7. Donelli, M., "Design of broadband metal nanosphere antenna arrays with a hybrid evolutionary algorithm," *Optics Letters*, Vol. 38, No. 4, 401–403, 2013.
8. Donelli, M. and P. Febvre, "An inexpensive reconfigurable planar array for Wi-Fi applications," *Progress In Electromagnetics Research C*, Vol. 28, 71–81, 2012.
9. Moriyama, T., M. Manekiya, and M. Donelli, "A compact switched-beam planar antenna array for wireless sensors operating at Wi-Fi band," *Progress In Electromagnetics Research C*, Vol. 83, 137–145, 2018.
10. Lalbakhsh, A., M. U. Afzal, K. Esselle, and S. L. Smith, "Wideband near-field correction of a Fabry-Perot resonator antenna," *IEEE Transactions on Antennas and Propagation*, Vol. 67, No. 3, 1975–1980, 2019.
11. Lalbakhsh, A., M. U. Afzal, and K. Esselle, "Simulation-driven particle swarm optimization of spatial phase shifters," *2016 International Conference on Electromagnetics in Advanced Applications*, 428–430, 2016.

12. Jamshidi, M., A. Lalbakhsh, S. Lotfi, H. Siahkamari, B. Mohamadzade, and J. Jalilian, "A neuro-based approach to designing a Wilkinson power divider," *International Journal of RF and Microwave Computer-Aided Engineering*, e22091, 2019.
13. Lalbakhsh, A., M. U. Afzal, K. Esselle, and B. Zeb, "Multi-objective particle swarm optimization for the realization of a low profile bandpass frequency selective surface," *ISAP*, 1–4, 2015.
14. Li, L., J. Wang, H. Ma, M. Feng, M. Yan, J. Zhang, and S. Qu, "All-dielectric metamaterial band stop frequency selective surface via high-permittivity ceramics," *2016 Progress In Electromagnetic Research Symposium (PIERS)*, 3324–3326, Shanghai, China, Aug. 8–11, 2016.
15. Lalbakhsh, A., M. U. Afzal, K. Esselle, and S. Smith, "Design of an artificial magnetic conductor surface using an evolutionary algorithm," *ICEAA*, 885–887, 2017.
16. Densmore, A. and Y. Rahmat-Samii, "Three-parameter elliptical aperture distributions for sum and difference antenna patterns using particle swarm optimization," *Progress In Electromagnetics Research*, Vol. 143, 709–743, 2013.
17. Jamshidi, M., A. Lalbakhsh, B. Mohamadzade, H. Siahkamari, and S. M. Mousavi, "A novel neural-based approach for design of microstrip filters", *AEU — International Journal of Electronics and Communications*, Vol. 110, 152847, 2019.
18. Haupt, R. L. and D. H. Werner, *Genetic Algorithms in Electromagnetics*, Wiley Inter-Science, 2007.
19. Khalid, A., S. A. Sheikh, I. H. Shah, and Q. U. Khan, "Synthesis of linear antenna array using genetic algorithm to reduce peak sidelobe level," *2015 9th International Conference on Electrical and Electronics Engineering (ELECO)*, 346–350, 2015.
20. Song, J., H. Zheng, and L. Zhang, "Application of particle swarm optimization algorithm and genetic algorithms in beam broadening of phased array antenna," *2010 International Symposium on Signals, Systems and Electronics*, Vol. 1, 1–4, 2010.
21. Le, Q. T., N. D. Nguyen, and T. T. Dam, " Amplitude and phase adaptive nulling with a genetic algorithm for array antennas," *2011 2nd International Conference on Artificial Intelligence, Management Science and Electronic Commerce*, 1887–1890, 2011.
22. Zhu, X., Q. Yang, M. Li, B. Liu, X. Yang, P. Chen, and B. Yang, "A circularly polarized waveguide slot array antenna based on genetic algorithm," *Proceedings of 2012 5th Global Symposium on Millimeter-Waves*, 155–158, 2012.
23. Yang, J. and P. S. Kildal, "Optimization of large log-periodic dual-dipole antenna by using Genetic Algorithm on embedded element in small log-periodic array," *2009 3rd European Conference on Antennas and Propagation*, 1308–1311, 2009.
24. Zeghdoud, A., M. C. Derbal, and M. Nedil, "Optimization of a dual-band microstrip antenna array using genetic algorithms," *2018 IEEE International Symposium on Antennas and Propagation & USNC/URSI National Radio Science Meeting*, 1005–1006, 2018.